



## Sea state bias in altimeter sea level estimates determined by combining wave model and satellite data

N. Tran,<sup>1</sup> D. Vandemark,<sup>2</sup> S. Labroue,<sup>1</sup> H. Feng,<sup>2</sup> B. Chapron,<sup>3</sup> H. L. Tolman,<sup>4</sup> J. Lambin,<sup>5</sup> and N. Picot<sup>6</sup>

Received 25 May 2009; revised 29 September 2009; accepted 6 October 2009; published 19 March 2010.

[1] This study documents a method for increasing the precision of satellite-derived sea level measurements. Results are achieved using an enhanced three-dimensional (3-D) sea state bias (SSB) correction model derived from both Jason-1 altimeter ocean observations (i.e., sea state and wind) and estimates of mean wave period from a numerical ocean wave model, NOAA's WAVEWATCH III. A multiyear evaluation of Jason-1 data indicates sea surface height variance reduction of  $1.26 (\pm 0.2) \text{ cm}^2$  in comparison to the commonly applied two-parameter SSB model. The improvement is similar for two separate variance reduction metrics and for separate annual data sets spanning 2002–2004. Spatial evaluation of improvement shows skill increase at all latitudes. Results indicate the new model can reduce the total Jason-1 and Jason-2 altimeter range error budgets by  $\sim 7.5\%$ . In addition to the 2-D (two-dimensional) and 3-D model differences in correcting the range for wavefield variability, mean model regional differences also occur across the globe and indicate a possible 1–2 cm gradient across ocean basins linked to the zonal variation in wave period (short fetch and period in the west, swells and long period in the east). Overall success of this model provides first evidence that operational wave modeling can support improved ocean altimetry. Future efforts will attempt to work within the limits of wave modeling capabilities to maximize their benefit to Jason-1 and Jason-2 SSB correction methods.

**Citation:** Tran, N., D. Vandemark, S. Labroue, H. Feng, B. Chapron, H. L. Tolman, J. Lambin, and N. Picot (2010), Sea state bias in altimeter sea level estimates determined by combining wave model and satellite data, *J. Geophys. Res.*, 115, C03020, doi:10.1029/2009JC005534.

### 1. Introduction

[2] The sea state bias (SSB) in ocean altimetry refers to the cm-level range adjustment applied to improve satellite radar estimation of mean sea level. The first-order SSB predictor,  $\varepsilon$ , is the height of the dominant gravity waves and can be written as  $\varepsilon(m) = \beta * \text{SWH}$ , where SWH is significant wave height and where  $\beta$  is  $O(0.03$  or  $3\%)$ . Most remaining variability and uncertainty in  $\beta$  resides in a term called the electromagnetic (EM) bias [e.g., Chelton *et al.*, 2001], arising in simplest terms because the radar altimeter power backscattered from wave troughs is enhanced over that from wave crests.

[3] Despite many field observation and modeling efforts, unresolved complexities in the interactions between radar

scattering and gravity wave elevation and slope dynamics dictate the continued reliance upon empirical satellite-based SSB estimation to develop the operational models. These empirical formulations have been refined in the past decade using a nonparametric statistical estimation approach [Gaspar *et al.*, 2002], but a recognized limitation is that the correction is solely determined by SWH and surface wind speed ( $U$ ) data. These two variables are chosen pragmatically because they are readily obtained from the satellite altimeter itself. However, it is expected that SSB uncertainty can be lowered if additional and accurate information on the instantaneous surface wavefield are obtained and applied as indicated by several nonsatellite field studies [Millet *et al.*, 2003, Melville *et al.*, 2004]. This task is a key remaining challenge for SSB improvement.

[4] This study presents a new multidimensional satellite SSB model where ocean wave period data are used within a three-input estimator. The mean gravity wave period ( $T_m$ ) estimates come from a numerical wind-wave model, NOAA's WAVEWATCH III (NWW3) [Tolman *et al.*, 2002]. The impetus for this approach stems from recent works examining NWW3 data application to the SSB problem [Feng *et al.*, 2006; Tran *et al.*, 2006]. In particular, Tran *et al.* [2006] showed that when using global satellite and wave model data, SSB estimation improvement is

<sup>1</sup>Space Oceanography Division, CLS, Ramonville St-Agne, France.

<sup>2</sup>Ocean Process Analysis Laboratory, University of New Hampshire, Durham, New Hampshire, USA.

<sup>3</sup>Space Oceanography Laboratory and Centre de Brest, IFREMER, Plouzané, France.

<sup>4</sup>Marine Modeling and Analysis Branch, EMC, NCEP, NOAA, Camp Springs, Maryland, USA.

<sup>5</sup>SI, DCT, CNES, Toulouse, France.

<sup>6</sup>PO, DCT, CNES, Toulouse, France.

regionally obtained when using two different wavefield statistical parameters. The first is the swell amplitude component of the total sea state ( $H_{\text{swell}}$ ) partitioned using *Hanson and Phillips* [2001] formulation and the second is the mean wave period defined as

$$T_m = m_0/m_1, \quad (1)$$

$$m_x = \int \int S(f, \theta) f^x df d\theta, \quad (2)$$

where  $m_x$  represents the respective statistical moments derived from the directional wave elevation density spectrum  $S(f, \theta)$ , with frequency  $f$  and wave propagation direction  $\theta$ . These findings were consistent with studies indicating that wave age, or the overall degree of wave development, measurably impacts the mean wavefield steepness and hence the EM bias dynamics [*Fu and Glazman*, 1991; *Minster et al.*, 1992; *Glazman et al.*, 1996; *Chapron et al.*, 2001; *Millet et al.*, 2003; *Melville et al.*, 2004].

[5] A basic illustration of the Jason-1 altimeter range bias explained by the NWW3 mean wave period using on-orbit data is supplied in Figure 1. It presents simple bin-averaged values of the altimeter sea level anomaly (SLA) data, without any SSB model correction (see equation (4)), for a given (SWH,  $U$ ) data subset with respect to  $T_m$ . Results show more than 3 cm of variation (i.e., 1% of SWH) across a wave period range of 6.5–9 s. Since the current working estimate of operational SSB model error is given as  $O(1\%)$  [*Chelton et al.*, 2001], this finding appears significant. A nearly linear relationship is displayed and the SSB magnitude is much larger for short period (associated to steeper young seas) than for long period (i.e., sinusoidal older seas) waves.

[6] While  $T_m$  is not the sole wavefield statistic pertinent to gravity wave impacts on the altimeter electromagnetic bias, this study will focus on removing the observed  $T_m$  dependence by developing an empirical multidimensional SSB model. The central study objective is to quantify the positive impact that wave model data can have on altimeter sea level data quality by combined use of NWW3 and Jason-1 altimeter data. The new satellite correction model is developed using a known two-dimensional (2-D) SSB nonparametric estimation approach revised to include three terms (SWH,  $U$ ,  $T_m$ ). Its skill will be compared to that of the standard 2-D model (i.e., based solely on SWH and  $U$ ) developed in the same manner and with the same data sets.

## 2. Methods

[7] NWW3 was run on a global  $1^\circ \times 1^\circ$  grid at a 6 hourly time step, without assimilation of altimeter wave height and forced with synoptic winds from the European Centre for Medium-Range Weather Forecasts (ECMWF). Further details about the combined NWW3/Jason-1 data set can be found by *Tran et al.* [2006]. Changes in the modeling approach, compared to the one used in the 2006 study include extending the nonparametric statistical model to three dimensions and expanding model validation by adding

an assessment that uses collinear (10 days) range measurement differences.

[8] Following *Labroue et al.* [2004], we derive an on-orbit SSB model from the input data vector  $\mathbf{x}$  using the formulation

$$\varepsilon = \varphi(\mathbf{x}, \theta), \quad (3)$$

where  $\varepsilon$  is the SSB (in cm),  $\varphi$  is a mapping function, and  $\theta$  holds the scalar constants for the equation. A kernel smoothing nonparametric approach [*Gaspar and Florens*, 1998; *Gaspar et al.*, 2002] is used to solve equation (3). Following recent studies [*Vandemark et al.*, 2002; *Labroue et al.*, 2004; *Tran et al.*, 2006] we develop a solution for  $\varepsilon$  by directly relating the altimeter SLA data, derived from a sea surface height (SSH') uncorrected for SSB, to input data vector  $\mathbf{x}$  as

$$\text{SLA}(\mathbf{x}) = \text{SSH}'(\mathbf{x}) - \text{MSL}(\mathbf{x}) = \varepsilon(\mathbf{x}) + \sigma(\mathbf{x}). \quad (4)$$

[9] MSL represents the mean sea surface level consisting of a decade-long average [*Hernandez and Schaeffer*, 2001] that enfolds both the geoid and mean dynamic topography while  $\sigma$  is a noise term combining all standard sea surface height correction errors (e.g., tides, high-frequency barotropic effect, ionospheric delay, water vapor, etc.) plus the time-varying sea surface topography. The key assumption of this approach is that under sufficient averaging  $\sigma(\mathbf{x}_j)$  will tend to zero for each specific combination ( $j$ ) of the input variables leaving a direct relationship between the dependent data and  $\varepsilon$ . In our study, the vector  $\mathbf{x}$  data set is formed using millions of coincident samples of SWH,  $U$ , and  $T_m$ ; the first two variables taken directly from the Jason-1 altimeter and the latter from the wave model data interpolated in space and time to coincide with each altimeter measurement. The extension of a satellite-based SSB NP solution to include a third input has not been accomplished before. However, increasing the input vector dimensions is straightforward [e.g., *Millet et al.*, 2003] and primarily requires a computational increase and a sufficiently large amount of measurements. For this study the same local-linear kernel smoothing approach (including kernel and adaptive bandwidth) is kept from *Tran et al.* [2006] and the model now solved for the three-dimensional (3-D) vector  $\mathbf{x} = (\text{SWH}, U, T_m)$ . We developed a solution resulting in a 3-D lookup table that describes the SSB behavior over 0–13 m in SWH, 0–25 m/s in  $U$ , and 0–18 s in  $T_m$ . Models were generated using 1 complete year of data, typically  $\sim 16$  million samples, for each of the years: 2002, 2003, and 2004. Observed model differences between these solutions are small, below cm levels, and we principally discuss the year 2002 solution in this paper. Next, as a means to the most direct evaluation of improvement gained by extending the SSB model to higher dimensions, a benchmark 2-D SSB algorithm is also computed on the basis of the standard altimeter SWH and  $U$  inputs and from the same Jason-1 data sets and using the same NP methods.

[10] Our use of the direct SLA method [*Vandemark et al.*, 2002] as recalled in equation (4) does differ from the two alternative SSB approximation approaches. These methods

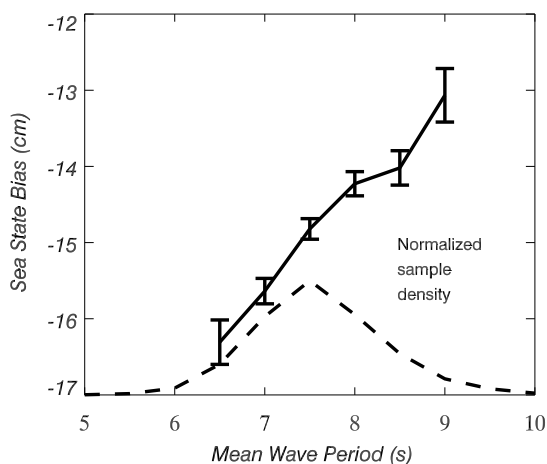


**Figure 1.** Average altimeter sea state bias (SSB) estimates versus mean wave period determined from Jason-1 sea level anomaly (SLA) observations (without application of SSB correction) where SWH is fixed at 3.2 m ( $\pm 0.1$ ) and  $U$  is fixed at  $9.5 \text{ ms}^{-1}$  ( $\pm 1.0$ ). The result includes 156,200 samples from 2002 to 2004 and 95% confidence intervals are shown. A normalized probability density function for the mean wave period (dashed line) is also provided.

use elevation differences calculated at fixed locations and between two successive satellite measurement times: over the Jason-1 10 days satellite repeat pass period for the collinear approach and over shorter periods of 3–5 days for the satellite pass crossover approach [Labroue *et al.*, 2004]. In these indirect calculation approaches, the relatively short time lapse between  $t_1$  and  $t_2$  and fixed location range differencing allows near isolation of the SSB as follows:

$$\Delta\text{SSH} = \text{SSH}_2^t - \text{SSH}_1^t = \varepsilon(t_2) - \varepsilon(t_1) + \gamma. \quad (5)$$

[11] Labroue *et al.* [2004] evaluated both the direct and indirect (SSH differences) methods and found that similar

SSB solutions are achieved even though the processes determining if  $\sigma$  and  $\gamma$  tend to zero are not equivalent. On the basis of that work, either approach is deemed reasonable for this study. Numerically, it is significantly more straightforward to implement the direct approach for NP estimation when including higher dimensional inputs and therefore this study uses the direct method.

[12] The chosen approach for model comparison follows from Tran *et al.* [2006]. 3-D model assessment against 2-D and 1-D SSB benchmarks will be performed using the recognized standard metric for comparing SSB models, i.e., calculation of the total variance reduction in the derived SSH after application of these specific SSB models. Results are gathered in Table 1. It is recognized that this test and the empirical methods for SSB modeling are each imperfect solutions for model determination and validation. For example, one disadvantage of the direct SSB model solution is the possibility that data sparseness in certain portions of the 2-D and 3-D input data domains will lead to ineffective removal of the dynamic topography under averaging in equation (4). While a full year of data is deemed adequate to create the direct SSB model for study objectives, we also address such concerns in two ways in the validation. First, the variance reduction metrics are evaluated over several complete-year data sets. This insures independence between the data used in SSB model creation and validation, i.e., the year 2002-version solutions are evaluated not only using 2002 measurements but also with 2003 and 2004 altimeter SSH data. Results from the 2004 version of the models are also provided for comparison. A second step is added both because of the familiarity in the SSB community of working with collinear and crossover differences and to expand confidence in validating this new three-input SLA SSB solution; we include a separate 2-D and 3-D model SSB assessment of the SSH variance reduction by using equation (5) with 10 days repeat pass Jason-1 difference data. This is a variance reduction calculation using the direct SSB model inserted into equation (5), not a calculation of yet another SSB model using collinear methods. If one observes relative consistency of results between these metrics then this provides further support

**Table 1.** Magnitude of Variance Reduction Obtained With the Common 2-D and the New 3-D SSB Correction Models Relative to the Reduction Obtained When Applying a 1-D SSB Correction<sup>a</sup>

Jason-1 SSB Models	Relative SLA Variance Reduction ( $\text{cm}^2$ )			Relative Collinear $\Delta\text{SSH}$ Variance Reduction ( $\text{cm}^2$ )		
	Validation Data Set			Validation Data Set		
	2002	2003	2004	2002	2003	2004
2002 version, 2-D SSB	1.37	1.62	1.88	2.80	2.98	3.20
2002 version, 3-D SSB	2.83	2.65	3.26	4.18	4.51	4.82
2002 version, difference (3-D–2-D)	1.46	1.03	1.38	1.38	1.53	1.62
2004 version, 2-D SSB	1.32	1.72	2.06	2.79	2.97	3.26
2004 version, 3-D SSB	2.47	2.74	3.56	3.89	4.33	4.74
2004 version, difference (3-D–2-D)	1.15	1.02	1.50	1.10	1.36	1.48
	SLA w/o SSB ( $\text{cm}^2$ )			Collinear $\Delta\text{SSH}$ w/o SSB ( $\text{cm}^2$ )		
Total variance	120.99	121.08	118.72	82.22	83.97	81.90
Variance explained by 1-D SSB	22.55	23.48	21.88	18.94	18.37	17.24

<sup>a</sup>Each estimate is for a full year of global Jason-1 altimeter data. The results are calculated using both the Jason-1 sea level anomaly (SLA) and collinear (10 days) sea surface height (SSH) difference data sets for the years indicated. Models were developed using year 2002 or 2004 data as indicated. Also provided are the total variance of both SLA and SSH differences without (w/o) sea state bias (SSB) correction and the variance explained by the 1-D SSB model computed as  $-3.8\%$  SWH.

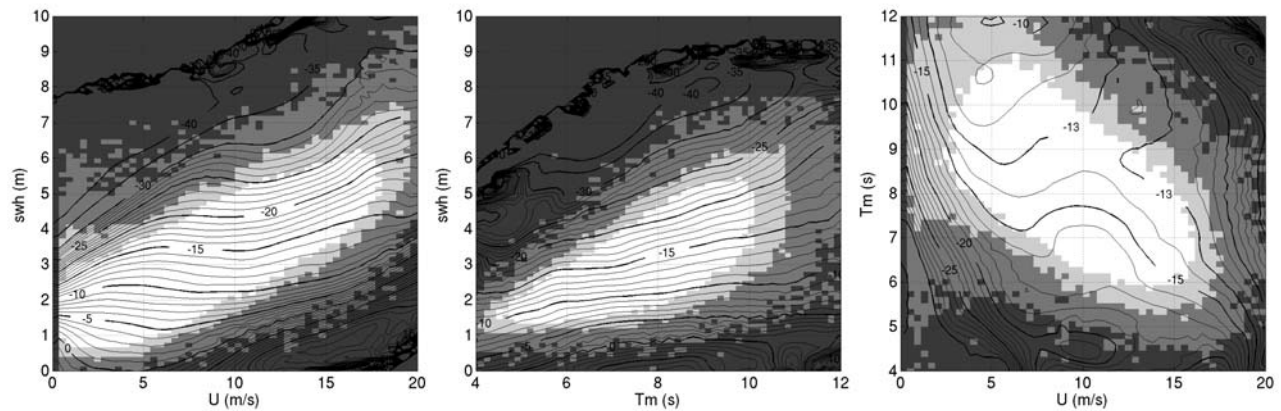


**Figure 2.** New 3-D Jason-1 SSB estimator as a function of significant wave height (SWH),  $U$ , and  $T_m$ . This is shown using three 2-D arrays with the respective third variable held constant. From left to right, these fixed values are  $T_m = 8.4$  s,  $U = 9.5$  m/s, and  $SWH = 3.2$  m. Isopleths represent a given SSB value (units in cm). Shaded areas represent data density with darkest gray holding no data, medium gray less than 20 samples, lighter shade less than 100, and the white region exceeding 100 samples per bin. The model is produced using all data in the year 2002.

that model inaccuracies lie significantly below the level of improvements gained. We note the primary study objective is to provide a method and solution for an improved SSB model and not to attain a final operational model validated under all conditions.

### 3. Results and Discussion

[13] Range error related to wind and sea state dynamics as predicted by the new 3-D Jason-1 altimeter model is shown in Figure 2. This model is developed with 1 year of satellite and model data from year 2002. The corrections are presented as familiar 2-D grids [cf. *Gaspar et al., 2002*] with contours given in cm. The fixed value of the third parameter for each part in Figure 2 is indicated in the caption. Shading denotes the available sample density across each 2-D data domain. Figure 2 (left) can be directly compared to the Jason-1 2-D model by *Labroue et al. [2004]* (their Figure 9) and agrees closely. Figure 2 (middle) and Figure 2 (right) illustrate that SSB also varies systematically with  $T_m$ . Figure 2 (middle) in the data-rich region shows a 3–4 cm variation versus  $T_m$  at a value of  $SWH = 3.2$  m, with bias magnitude decreasing as the wave period increases. This result is consistent with Figure 1, and an  $O(1\%)$  SWH variation is apparent at most SWH values in Figure 2 (middle). Nonlinear variation of the SSB versus dependent variables is evident in all parts and validates the use of the kernel smoothing model approach.

[14] As with previous satellite SSB studies, we use altimeter sea surface height variance reduction metrics to assess model performance. The main objective is to determine if the 3-D correction model is able to reduce variance in sea level measurements relative to the present-day standard 2-D approach. For completeness, we present results from two different validation metrics: (1) variance reduction in the altimeter-derived SLA using candidate SSB models and (2) variance reduction in the 10 days differenced SSH obtained from along track satellite repeat passes (collinear differences, equation (5)).

[15] Results for 1 year global estimates are provided in Table 1. For both methods, evaluations are performed after applying 1-D, 2-D, and 3-D SSB model corrections. The explained variance is given with respect to a 1-D benchmark SSB model [*Tran et al., 2006*] where positive numbers indicate enhanced magnitude in correction skill ( $\text{cm}^2$ ). The 2-D Jason-1 model is built using altimeter SWH and  $U$  as discussed earlier. As part of sensitivity tests for this study we have produced SSB models using 1 year of data from two separate years (2002 and 2004) and are evaluating them against data in years 2002–2004.

[16] Model enhancement is most clearly seen in Table 1 by examining differences between the 3-D and 2-D variance reduction. Also provided are the total variance of both SLA and SSH differences without SSB correction and the variance explained by the 1-D SSB model as reference marks. The change from 2-D to 3-D model consistently provides more than  $1 \text{ cm}^2$  improvement with values as high as  $1.6 \text{ cm}^2$ . The improvements are nearly equivalent for SSB models developed using 2002 or 2004 data, with all values agreeing to better than  $0.3 \text{ cm}^2$ . The same holds for the absolute 2-D and 3-D SSB reduction values for the 2002 and 2004 models. The largest variability in the 3-D–2-D difference is from year to year, with 2003 SLA values being smallest, but these values remain above  $1 \text{ cm}^2$ . The average of the six values based on SLA ( $1.26 \pm 0.2 \text{ cm}^2$ ) translates to 1.12 cm in root-mean-square (RMS) sea level estimate improvement as a result of this new model compared to a model developed using only SWH and  $U$ .

[17] Note that differences between the two separate metric estimators across Table 1 (e.g., 2-D SSB results across a given row) are assumed to be related to different yearly average of prevalent wind and sea state conditions but also to different mean values of SLA and collinear SSH differences over these 3 years. Since the interest is on relative SSB model performance within the separate metrics, the comparison results are consistent within each data set.

[18] Differences between these two variance-reduction metrics were expected since the variance of SLA and the

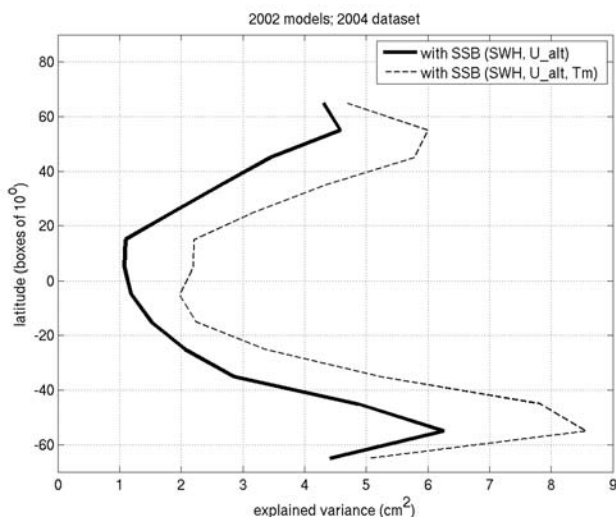


**Figure 3.** Variation with latitude of band-averaged sea surface height (SSH) variance ( $\text{cm}^2$ ) reduction (positive values) obtained using the 2-D and 3-D models in comparison to a 1-D ( $-3.8\%$  SWH) benchmark. Results are obtained by collinear analyses for year 2004 and derived using  $10^\circ$  latitude bands.

variance of collinear SSH differences do not encompass exactly the same geophysical content. Collinear repeat pass SSH differencing removes some possible correlation between the suite of altimeter corrections, the dynamic topography, and sea state that are contained in the SLA estimator. Moreover, the absolute RMS value at any location is much smaller than for the SLA and the relative SSB correction contributions (2-D and 3-D) may well differ and be enhanced in the collinear calculations. Table 1 shows that while the relative differences of 2-D and 3-D SSB impacts versus the 1-D benchmark are slightly larger for the collinear versus the SLA metric, the row three average of 3-D–2-D differences ( $1.41$  versus  $1.26 \text{ cm}^2$ ) are nearly equal and thus the positive impact of wave period data due to the 3-D SSB model is unambiguous in both tests. Overall, while Table 1 data only provide simple single year estimates of performance, one sees that the 3-D model consistently indicates positive impact and that results are nearly insensitive to changes in the data period used to train the model. Year to year variation in these results is slightly larger but this is still small ( $<0.3 \text{ cm}^2$ ) compared to the improvement, and a likely source for these dynamics is temporal variability in the actual wind and wavefields in these years.

[19] Figure 3 expands beyond a single global value to further examine model performance. Results show variance reduction due to 2-D and 3-D SSB models versus the 1-D benchmark with respect to latitude and using year 2004 collinear  $\Delta\text{SSH}$  Jason-1 measurements (from SSB models trained with 2002 data). It is apparent that the 3-D model provides an enhanced correction at all latitudes. The improvement often exceeds  $1.0 \text{ cm}^2$ , especially at high latitudes where SWH values are larger. Comparisons along latitude show that the 3-D value is typically a factor of 1.4–1.6 greater than the 2-D SSB explained variance. The improvement at all latitudes can be seen as a large improvement compared to any of the candidate 2-D SSB models

developed by *Tran et al.* [2006] (cf. their Figure 4), thus demonstrating that retaining both the SWH and  $U$  from the actual altimeter and adding a wave model parameter into a 3-D estimator leads to increased performance.

[20] Results in Figure 4 further illustrate the impact of  $T_m$  in the SSB correction showing a global map of annually averaged differences between 2-D and 3-D SSB models, presenting both the mean and variance. Clear spatial patterns emerge. One sees highest positive mean differences can exceed  $1 \text{ cm}$  along the western edges of the ocean basins while negative values are found to the east. Nearly continuous zonal gradients are apparent across each ocean basin in both the mean and variance differences. We attribute these features to the zonal gradient in mean wave period distributions, with known dominance of long-period swell in the west and limited fetch and shorter-period waves prevailing in the east [Young, 1999; Chen et al., 2002; Tran et al., 2006; Alves, 2006]. This systematic variation in the wave period can be contrasted with the known meridional gradient in both wave height and wind speed where higher wind and waves most frequently occur at highest latitudes.

[21] Results in Figure 4 also highlight that one possible ramification of this 3-D SSB correction would be the alteration of the mean sea surface [Hernandez and Schaeffer, 2001] and mean dynamic topography (MDT) [Rio and Hernandez, 2004] derived using long-term altimetry missions. These altimeter-influenced products assume that the 2-D SSB model is accurate and is consistently applied within a multiyear average. Figure 5 provides one slice across the 3-D–2-D difference map of Figure 4 (top). Here one sees a nearly linear  $1\text{--}2 \text{ cm}$  difference between the 2-D and 3-D models across the middle latitude in the North Pacific and North Atlantic driven by  $T_m$  variation. A review of recent work attempting to measure the global MDT by combining surface current drifters, geoid measurements, and altimetry [Vossepoel, 2007; Maximenko et al., 2009] has shown: (1) zonal SSH gradients are of order  $80\text{--}200 \text{ cm}$  across basin at middle latitudes in the northern hemisphere and (2) error in estimation methods are  $4\text{--}5 \text{ cm}$  RMS in low-current regions and  $10\text{--}15 \text{ cm}$  in higher-current regions. The  $1\text{--}2 \text{ cm}$  cross basin gradient due to an SSB

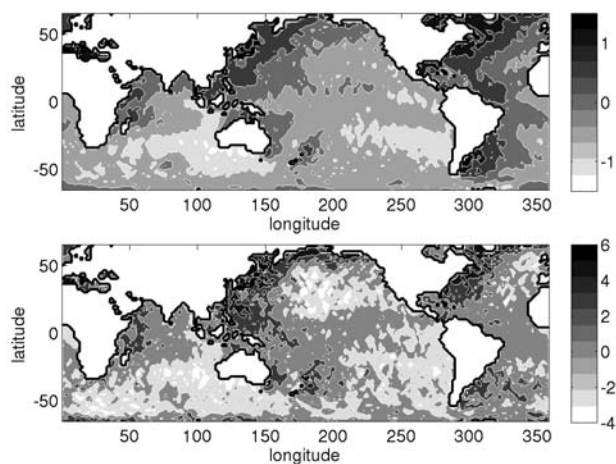


**Figure 4.** Maps of (top) annual average of the difference (2-D–3-D) between the two models (in cm) and (bottom) variance difference (3-D–2-D) between the models.

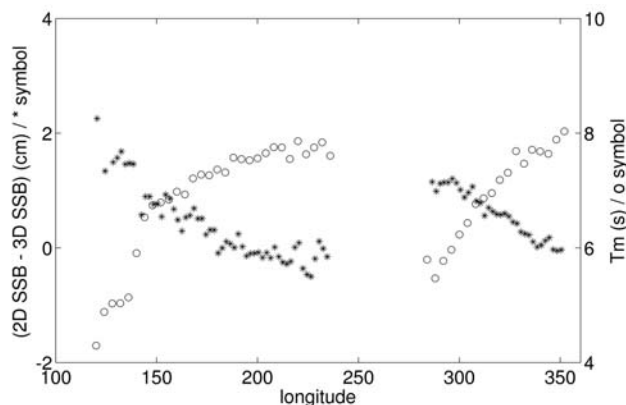


**Figure 5.** Annual average of SSB estimate differences between the two models across the North Pacific and North Atlantic at about 39°N (extracted from Figure 4 (top)). They are compared with mean wave period  $T_m$  variation.

model change would then be  $O(1\%–2\%)$  and this would be both in the MDT and in any derived meridional geostrophic current, and translates grossly in an absolute velocity error below 0.2 cm/s. Combining the small impact with the fact that this systematic 1–2 cm SSB effect lies well below the present MDT detection limits suggests these concerns are of second order at this time.

[22] One further means to quantify this study’s implication is to insert the average 1.12 cm RMS improvement of Table 1 into the overall altimeter measurement error budget. The SSB uncertainty estimate used in these budgets is typically  $\sim 1\%$  of SWH which translates to 2.3 cm of uncertainty at the global median SWH value of 2.3 m. While such a single number estimate does not fully enfold the global range of SWH and SSB dynamics that increase with latitude as in Figure 3, a 1.12 cm reduction applied to 2.3 cm amounts to a 12.6% improvement. Table 1 of Vincent *et al.* [2003] calculates the Jason-1 altimeter range estimate uncertainty to be 2.95 cm RMS at SWH = 2 m. This includes ionospheric, atmospheric, and wave corrections. Inserting the SSB improvement into that budget lowers the total mark to 2.73 cm, a  $\sim 7.5\%$  improvement in the total range measurement uncertainty budget. Note that use of filtered SWH when computing the SSB correction values in the operational chain would also reduce the amount of range estimate uncertainty coming from the SSB term. Indeed similarly to the dual-frequency ionospheric correction which is filtered over 100 km in the Jason-2 products, the along-track SSB values would be smoother. The SWH filtering could consist in along-track averaging of the 1 Hz SWH data over a 40–100 km (to be determined) ground segment in order to reduce sporadic noise in the SWH data which do not always look physical.

[23] Finally, as another component of this investigation and while not shown here, a separate 3-D SSB model was also developed by replacing  $T_m$  with a variable related to the amplitude of swell ( $H_{\text{swell}}$ ) defined as

$$H_{\text{swell}} = 4 \sqrt{m_0 - \int_{f_{\text{bp}}}^{f_4} \int S(f, \theta) df d\theta}, \quad (6)$$

where  $f_4 = 0.4$  Hz and  $f_{\text{bp}}$  is the spectral frequency just below the wind sea spectral peak at the half power point in the wind sea spectral density [Hanson and Phillips, 2001].

[24] This model was developed in part because of work in Tran *et al.* [2006] indicating that  $H_{\text{swell}}$  data are another candidate for improved global scale SSB modeling. The swell-informed 3-D model slightly but consistently outperforms this study’s  $T_m$  3-D model at latitudes below 20° (improvement of 0.1–0.3 cm<sup>2</sup>), but at high latitudes it underperforms and can even revert to 2-D model levels. As evident in Table 1, 0.3 cm<sup>2</sup> is also near the confidence level of estimate evaluations. Still, the ubiquity and frequent dominance of swell in the tropics, its modeling, and its impact on the SSB should not be neglected. Future work will look at both higher-dimensional SSB models and the possibility of more regionally focused corrections. However, in keeping with the objective of this paper, we assert that the comprehensive and robust improvement obtained solely using  $T_m$  provides evidence that ocean wave model data, in this case longer wave information related to the mean spectral wave number  $\langle k \rangle$ , can be used to improve the precision of altimeter sea level measurements.

#### 4. Conclusion

[25] This study was built under the assumption that the wave-dependent range bias in satellite altimetry can be improved by the inclusion of ocean wavefield data taken from a global hindcast model. Mean wave period estimates from the NOAA’s WAVEWATCH III wind-wave prediction system are combined with Jason-1 altimeter sea state and wind speed estimates to develop a new SSB model and quantify its impact. Results show reduced sea surface height variance both at global and regional scale. This is obtained when comparing to the accepted standard two-dimensional altimeter SSB correction that uses only altimeter measurements. Both the 2-D and 3-D models were produced using the same SLA data (year 2002 or 2004) and nonparametric estimation method to insure clear demonstration of wave model data impacts. Results of Table 1 and Figure 4 indicate comprehensive improvement with a global 3-D SSB model where a single value global variance gain estimate is 1.26 ( $\pm 0.2$ ) cm<sup>2</sup>, or 1.12 cm in RMS. While this value may appear small, the average improvement is of order 0.13% in SWH (the global mode SWH is 2.3 m), a considerable value given that the two parameter model uncertainty is near 1% SWH. Moreover, as each of the precision mission ocean altimeter correction terms are refined, this  $O(1$  cm) improvement is comparable to or greater than those recently achieved in revised orbits, water vapor, and high-frequency barotropic model modifications [e.g., Beckley *et al.*, 2007; Carrere and Lyard, 2003]. We estimate the improvement at 7.5% in the total range error for the Jason-1 altimeter and this should similarly apply for the presently orbiting Jason-2 altimeter. Perhaps most notably, this study provides a gain in global SSB variance reduction that has not been previously achieved through many attempts that have dealt solely with use of the two altimeter measurements of SWH and  $U$ .

[26] There are several caveats to mention and key issues to address in the near future pertaining to this work. First, the error and resolution limitations of wavefield estimates taken from a wave model must be recognized. For this study

data set, the agreement between altimeter and wave model SWH was better than 0.2 m RMS and for altimeter and model wind speed, better than 1.5 m/s RMS. Validation of the full directional spectrum including swell mode amplitudes and directions are much harder to document and those aspects of the model more suspect [cf. Bidlot et al., 2007]. Thus an important near term issue is documenting uncertainty within SSB models and end product SSH data related to wave model uncertainty. And while the SSB approach here is primarily empirical, further sensitivity studies are underway to evaluate optimal use of wavefield parameters from WAVEWATCH-III used in 3-D and 4D SSB models including the mean wave number and swell field amplitude. Next, the direct or SLA bias determination method requires a significant amount of data increase in the data density (see Figure 4) to assure model accuracy in data poor areas of the 3-D domain. Therefore, we are also developing revised numerical inversion methods to handle very large multiyear data sets spanning 2002–2009. Finally, the same methods need to be applied to the Jason-2 and Topex/Poseidon altimeter mission data to insure that this empirically derived SSB approach is applicable to all data sets that are central to the long-term ocean circulation and sea level rise observations that now extend from 1993 onward.

[27] **Acknowledgments.** The authors wish to thank the two anonymous reviewers who provided valuable comments that lead us to produce a significantly more comprehensive paper than originally submitted. This work was performed within activities supported by the Centre National d'Etudes Spatiales (CNES) in France and the National Aeronautics and Space Administration (NASA).

## References

- Alves, J.-H. G. M. (2006), Numerical modelling of ocean swell contributions to the global wind-wave climate, *Ocean Modell.*, *11*, 98–122, doi:10.1016/j.ocemod.2004.11.007.
- Beckley, B. D., F. G. Lemoine, S. B. Luthcke, R. D. Ray, and N. R. Zelenka (2007), A reassessment of global and regional mean sea level trends from TOPEX and Jason-1 altimetry based on revised reference frame and orbits, *Geophys. Res. Lett.*, *34*, L14608, doi:10.1029/2007GL030002.
- Bidlot, J.-R., et al. (2007), Inter-comparison of operational wave forecasting systems, paper presented at 10th International Workshop of Waves Hindcasting and Forecasting, U.S. Army Eng. Res., Hawaii Kahuku, 11–16 November.
- Carrere, L., and F. Lyard (2003), Modeling the barotropic response of the global ocean to atmospheric wind and pressure forcing: Comparisons with observations, *Geophys. Res. Lett.*, *30*(6), 1275, doi:10.1029/2002GL016473.
- Chapron, B., D. Vandemark, T. Elfouhaily, D. R. Thompson, P. Gaspar, and S. Labroue (2001), Altimeter sea state bias: A new look at global range error estimates, *Geophys. Res. Lett.*, *28*, 3947–3950, doi:10.1029/2001GL013346.
- Chelton, D. B., J. C. Ries, B. J. Haines, L.-L. Fu, and P. S. Callahan (2001), Satellite altimetry, in *Satellite Altimetry and Earth Sciences*, *Int. Geophys. Ser.*, vol. 69, edited by L. Fu and A. Cazenave, pp. 1–131, Academic, San Diego, Calif.
- Chen, G., B. Chapron, R. Ezraty, and D. Vandemark (2002), A global view of swell and wind sea climate in the ocean by satellite altimeter and scatterometer, *J. Atmos. Oceanic Technol.*, *19*, 1849–1859, doi:10.1175/1520-0426(2002)019<1849:AGVOSA>2.0.CO;2.
- Feng, H., D. Vandemark, Y. Quilfen, B. Chapron, and B. Beckley (2006), Assessment of wind forcing impact on a global wind-wave model using the TOPEX altimeter, *Ocean Eng.*, *33*, 1431–1461, doi:10.1016/j.oceaneng.2005.10.015.
- Fu, L., and R. Glazman (1991), The effect of the degree of wave development on the sea state bias in radar altimetry measurement, *J. Geophys. Res.*, *96*, 829–834, doi:10.1029/90JC02319.
- Gaspar, P., and J.-P. Florens (1998), Estimation of the sea state bias in radar altimeter measurements of sea level: Results from a new nonparametric method, *J. Geophys. Res.*, *103*, 15,803–15,814, doi:10.1029/98JC01194.
- Gaspar, P., S. Labroue, F. Ogor, G. Lafitte, L. Marchal, and M. Rafanel (2002), Improving nonparametric estimates of the sea state bias in radar altimetry measurements of sea level, *J. Atmos. Oceanic Technol.*, *19*, 1690–1707, doi:10.1175/1520-0426(2002)019<1690:INEOTS>2.0.CO;2.
- Glazman, R., A. Fabrikant, and M. Srokosz (1996), Numerical analysis of the sea state bias for satellite altimetry, *J. Geophys. Res.*, *101*, 3789–3799, doi:10.1029/95JC03619.
- Hanson, J. L., and O. M. Phillips (2001), Automated analysis of ocean surface directional wave spectra, *J. Atmos. Oceanic Technol.*, *18*, 277–293, doi:10.1175/1520-0426(2001)018<0277:AAOOSD>2.0.CO;2.
- Hernandez, F., and P. Schaeffer (2001), The CLS01 Mean Sea Surface: A validation with the GSFC00.1 surface, *CLS Technical Note*, 14 pp. (Available at [http://www.aviso.oceanobs.com/fileadmin/documents/data/produits/auxiliaires/cls01\\_valid\\_mss.pdf](http://www.aviso.oceanobs.com/fileadmin/documents/data/produits/auxiliaires/cls01_valid_mss.pdf)).
- Labroue, S., P. Gaspar, J. Dorandeu, O. Z. Zanife, F. Mertz, P. Vincent, and D. Choquet (2004), Non-parametric estimates of the sea state bias for Jason-1 radar altimeter, *Mar. Geod.*, *27*, 453–481, doi:10.1080/01490410490902089.
- Maximenko, N., P. Niiler, M.-H. Rio, O. Melnichenko, L. Centurioni, D. Chambers, V. Zlotnicki, and B. Galperin (2009), Mean dynamic topography of the ocean derived from satellite and drifting buoy data using three different techniques, *J. Atmos. Oceanic Technol.*, *26*, 1910–1919, doi:10.1175/2009JTECHO672.1.
- Melville, W. K., F. C. Felizardo, and P. Matusov (2004), Wave slope and wave age effects in measurements of electromagnetic bias, *J. Geophys. Res.*, *109*, C07018, doi:10.1029/2002JC001708.
- Millet, F. W., D. V. Arnold, K. F. Warnick, and J. Smith (2003), Electromagnetic bias estimation using in situ and satellite data: 1. RMS wave slope, *J. Geophys. Res.*, *108*(C2), 3040, doi:10.1029/2001JC001095.
- Minster, J. F., D. Jourdan, C. Boissier, and P. Midol-Monnet (1992), Estimation of the sea state bias in radar altimeter Geosat data from examination of frontal systems, *J. Atmos. Oceanic Technol.*, *9*, 174–187, doi:10.1175/1520-0426(1992)009<0174:EOTSSB>2.0.CO;2.
- Rio, M.-H., and F. Hernandez (2004), A mean dynamic topography computed over the world ocean from altimetry, in situ measurements, and a geoid model, *J. Geophys. Res.*, *109*, C12032, doi:10.1029/2003JC002226.
- Tolman, H. L., B. Balasubramanian, L. D. Burroughs, D. V. Chalikov, Y. Y. Chao, H. S. Chen, and V. M. Gerald (2002), Development and implementation of wind generated ocean surface wave models at NCEP, *Weather Forecasting*, *17*, 311–333, doi:10.1175/1520-0434(2002)017<0311:DAIOWG>2.0.CO;2.
- Tran, N., D. Vandemark, B. Chapron, S. Labroue, H. Feng, B. Beckley, and P. Vincent (2006), New models for satellite altimeter sea state bias correction developed using global wave model data, *J. Geophys. Res.*, *111*, C09009, doi:10.1029/2005JC003406.
- Vandemark, D., N. Tran, B. D. Beckley, B. Chapron, and P. Gaspar (2002), Direct estimation of sea state impacts on radar altimeter sea level measurements, *Geophys. Res. Lett.*, *29*(24), 2148, doi:10.1029/2002GL015776.
- Vincent, P., S. D. Desai, J. Dorandeu, M. Ablain, B. Soussi, P. S. Callahan, and B. J. Haines (2003), Jason-1 geophysical performance evaluation, *Mar. Geod.*, *26*, 167–186, doi:10.1080/714044517.
- Vossepoul, F. C. (2007), Uncertainties in the mean ocean dynamic topography before the launch of the Gravity Field and Steady-State Ocean Circulation Explorer (GOCE), *J. Geophys. Res.*, *112*, C05010, doi:10.1029/2006JC003891.
- Young, I. R. (1999), Seasonal variability of the global ocean wind and wave climate, *Int. J. Climatol.*, *19*, 931–950, doi:10.1002/(SICI)1097-0088(199907)19:9<931::AID-JOC412>3.0.CO;2-O.

B. Chapron, Centre de Brest, IFREMER, F-29280 Plouzané, France.  
 H. Feng and D. Vandemark, Ocean Process Analysis Laboratory, University of New Hampshire, Durham, NH 03824, USA.  
 S. Labroue and N. Tran, DOS, CLS, 8-10 rue Hermes, F-31520 Ramonville St-Agne, France. (ntran@cls.fr)  
 J. Lambin, SI, DCT, CNES, F-31401 Toulouse, France.  
 N. Picot, PO, DCT, CNES, F-31401 Toulouse, France.  
 H. L. Tolman, Marine Modeling and Analysis Branch, EMC, NCEP, NOAA, Camp Springs, MD 20746, USA.